

# Black holes and Higgs stability

Nikolaos Tetradis

*Department of Physics, University of Athens, Zographou 157 84, Greece  
and*

*Physics Department, Theory Unit, CERN, CH-1211 Geneva 23, Switzerland*

## Abstract

We study the effect of primordial black holes on the classical rate of nucleation of AdS regions within the standard electroweak vacuum. We find that the energy barrier for transitions to the new vacuum, which characterizes the exponential suppression of the nucleation rate, can be reduced significantly in the black-hole background. A precise analysis is required in order to determine whether the the existence of primordial black holes is compatible with the form of the Higgs potential at high temperature or density in the Standard Model or its extensions.

# Contents

<b>1</b>	<b>Introduction</b>	<b>3</b>
<b>2</b>	<b>Matching the geometries</b>	<b>4</b>
<b>3</b>	<b>The critical bubbles</b>	<b>6</b>
<b>4</b>	<b>Higgs (in)stability</b>	<b>10</b>
<b>5</b>	<b>Numerical solutions</b>	<b>11</b>
<b>6</b>	<b>Summary and conclusions</b>	<b>15</b>
<b>A</b>	<b>Equation of motion</b>	<b>17</b>
<b>B</b>	<b>Bubble evolution in asymptotically flat space</b>	<b>19</b>
<b>C</b>	<b>Bubble evolution in asymptotically de Sitter space</b>	<b>22</b>

# 1 Introduction

The creation of an anti-de Sitter (AdS) bubble within asymptotically flat or de Sitter (dS) space is a problem relevant for the issue of vacuum decay. The nucleation of such a bubble can occur through quantum fluctuations within the false vacuum, with a rate that is exponentially suppressed by the action of the saddle point dominating the transition [1]. The creation is also possible during inflation, when massless fields fluctuate with a characteristic scale set by the almost constant Hubble parameter  $H_{\text{inf}}$ . This process can be viewed as a transition beyond the potential barrier in the direction of the true vacuum, which is induced by the effective Gibbons-Hawking temperature  $T = H_{\text{inf}}/2\pi$  [2]. A similar transition may occur after the end of inflation, during reheating, or in any period during which fluctuations become strong.

Through the above processes the Higgs field of the Standard Model can fluctuate towards values a few orders of magnitude below the Planck scale, for which its potential becomes deeper than for the standard electroweak vacuum [3, 4, 5, 6, 7]. Regions where the transition takes place can be considered as regions of AdS space within standard Minkowski or dS space. If they are approximated as spherically symmetric, their evolution becomes tractable analytically, along lines similar to [8]. The general conclusion is that the AdS bubbles expand and engulf the whole external Minkowski space, evolving into a singularity characterized as the AdS crunch [1, 7]. For bubbles created during inflation this catastrophic scenario can be avoided if  $H_{\text{inf}}$  is sufficiently small, so that fluctuations beyond the potential barrier are highly improbable [7].

It was pointed out recently [9] that the quantum nucleation of bubbles of true vacuum can be enhanced around black holes that act as impurities in the false vacuum. In the context of the Standard Model, the presence of black holes may destabilize the standard electroweak vacuum by reducing drastically the barrier for quantum fluctuations in the direction in which the Higgs potential becomes negative. The origin of the primordial black holes that are relevant for this issue lies in strong fluctuations in the early Universe, which affect the Higgs field as well. A question that arises naturally is whether the creation of black holes during inflation or during later periods is accompanied by the appearance of AdS bubbles around them that arise as classical fluctuations. In such a scenario, the transition to the true vacuum is not a quantum phenomenon, but is triggered by the high temperature or density environment.

A primordial black hole can form when the density fluctuations are sufficiently large for an overdense region to collapse [10]. Its maximal mass is of order the total mass within the particle horizon  $m_{\text{bh}} \sim M_{\text{Pl}}^2/H$ , while its maximal radius is  $R_{\text{bh}} \sim 1/H$ . These estimates are also valid for black holes that are pair-produced during inflation [11]. The presence of a significant number of primordial black holes today depends on their production rate, their dilution by the expansion and their evaporation rate. Black holes larger than roughly  $10^{15}$  gr can survive until the present time and play the role of dark

matter. The form of the Higgs potential places an additional constraint on the possible existence of primordial black holes: The creation of an AdS bubble around a typical black hole must be disfavored. In the opposite case, the Universe cannot evolve to its present form.

In the following we discuss the possible enhancement of classical instabilities of the standard electroweak vacuum near black holes. The relevant quantity, which is the focus of our analysis, is the height of the energy barrier between the standard vacuum and the region in which the Higgs potential becomes negative. The nucleation rate of the new phase is exponentially suppressed by the ratio of the energy barrier to the characteristic scale of fluctuations, such as the temperature or any other parameter determining the field dispersion.

In section 2 and appendices A-C we analyze the idealized problem of an AdS bubble with a black hole at its center, within asymptotically flat or dS space. We determine the ADM mass of the critical bubble, from which the energy barrier can be estimated. In section 3 we study the effect of the black hole on the critical-bubble mass. In section 4 we estimate the energy barrier using the energy scales of the Higgs potential. In section 5 we address the problem by solving numerically the equation of motion of the Higgs field in order to obtain the precise form of the bubble profile and the related energy barrier. The last section contains our conclusions.

## 2 Matching the geometries

An idealized setting in which our problem can be addressed consists of a spherical region of AdS-Schwarzschild space with a mass parameter  $m$ , separated by a thin shell from a Schwarzschild or dS-Schwarzschild exterior with a mass parameter  $M$ . The difference  $\delta M = M - m$  determines how the mass  $M$ , attributed by a faraway observer to this configuration, compares to the mass parameter  $m$ . The sign of  $\delta M$  is a first indicator of whether the “dressing” of a black hole by an AdS bubble is energetically favorable.

For an external observer, the presence of the bubble has a gravitational effect equivalent to the presence of a central mass. As a result, the exterior metric is of the Schwarzschild or dS-Schwarzschild type. We assume a spherical AdS-Schwarzschild interior, separated from the external space by a thin wall with constant surface tension  $\sigma$ . In the thin-wall approximation, the motion of the wall is determined by junction conditions that relate the extrinsic curvature on each of its sides [12]. The basic elements of the problem are:

1. The space inside the bubble has a metric

$$ds^2 = -f_{\text{in}}(r) d\eta^2 + \frac{dr^2}{f_{\text{in}}(r)} + r^2 d\Omega_2^2, \quad r < R, \quad (1)$$

with  $f_{\text{in}}(r) = 1 + r^2/\ell_{\text{AdS}}^2 - 2Gm/r$  and  $G = 1/(8\pi M_{\text{Pl}}^2)$ . The parameter  $m$  characterizes the black hole located at  $r = 0$ . For  $m = 0$  we obtain the standard AdS solution, expressed in global coordinates. The space has negative vacuum energy  $V_{\text{AdS}}$ , corresponding to the length scale  $1/\ell_{\text{AdS}}^2 = 8\pi G|V_{\text{AdS}}|/3$ .

2. The space outside the bubble is described by the metric

$$ds^2 = -f_{\text{out}}(r) dt^2 + \frac{dr^2}{f_{\text{out}}(r)} + r^2 d\Omega_2^2, \quad r > R, \quad (2)$$

with  $f_{\text{out}}(r) = 1 - r^2/\ell_{\text{dS}}^2 - 2GM/r$ . The positive vacuum energy  $V_{\text{dS}}$  is related to the length scale  $\ell_{\text{dS}}$  through  $1/\ell_{\text{dS}}^2 = 8\pi G V_{\text{dS}}/3$ . The parameter  $M$  corresponds to the mass assigned to the bubble by an asymptotic observer.

3. The two regions are separated by a domain wall with constant surface tension  $\sigma$ . The metric on the domain wall can be written as

$$ds^2 = -d\tau^2 + R^2(\tau) d\Omega_2^2, \quad (3)$$

where  $R(\tau)$  denotes the location of the wall in both coordinate systems (1) and (2). The evolution is expressed in terms of the proper time  $\tau$  on the wall. In the scenario of Higgs fluctuations produced during inflation,  $\sigma$  is induced by the kinetic and potential energy of the Higgs field.

The continuity of the metric gives

$$f_{\text{in}}(R) \dot{\eta} = \epsilon_1 \left( \dot{R}^2 + f_{\text{in}}(R) \right)^{1/2}, \quad (4)$$

$$f_{\text{out}}(R) \dot{t} = \epsilon_2 \left( \dot{R}^2 + f_{\text{out}}(R) \right)^{1/2}, \quad (5)$$

where  $\epsilon_1 = \pm 1$ ,  $\epsilon_2 = \pm 1$  are possible sign choices and a dot denotes a derivative with respect to  $\tau$ . We define a spacelike vector  $\xi^\mu$  orthogonal to the four-velocity of the wall, given by  $U_{\text{in}}^\mu = (\dot{\eta}, \dot{R}, \vec{0})$  and  $U_{\text{out}}^\mu = (\dot{t}, \dot{R}, \vec{0})$  in each of the frames. We have

$$\xi_{\text{in}}^\mu = \left( \frac{\dot{R}}{f_{\text{in}}}, f_{\text{in}} \dot{\eta}, \vec{0} \right) = \left( \frac{\dot{R}}{f_{\text{in}}}, \epsilon_1 (f_{\text{in}} + \dot{R}^2)^{1/2}, \vec{0} \right) \quad (6)$$

$$\xi_{\text{out}}^\mu = \left( \frac{\dot{R}}{f_{\text{out}}}, f_{\text{out}} \dot{t}, \vec{0} \right) = \left( \frac{\dot{R}}{f_{\text{out}}}, \epsilon_2 (f_{\text{out}} + \dot{R}^2)^{1/2}, \vec{0} \right). \quad (7)$$

The junction conditions connect the discontinuity in the extrinsic curvature to the surface tension [12]:

$$(K_{\text{out}})^i_j - (K_{\text{in}})^i_j = -4\pi G \sigma \delta^i_j. \quad (8)$$

They give

$$\epsilon_2 (f_{\text{out}} + \dot{R}^2)^{1/2} - \epsilon_1 (f_{\text{in}} + \dot{R}^2)^{1/2} = \beta_{\text{out}} - \beta_{\text{in}} = -4\pi G \sigma R. \quad (9)$$

The square of eq. (9) can be put in the form:

$$2GM = 2Gm + \left( \kappa^2 - \frac{1}{\ell_{\text{AdS}}^2} - \frac{1}{\ell_{\text{dS}}^2} \right) R^3 + 2\epsilon_2 \kappa R^2 \left( 1 - \frac{2GM}{R} - \frac{R^2}{\ell_{\text{dS}}^2} + \dot{R}^2 \right)^{1/2}, \quad (10)$$

with  $\kappa = 4\pi G\sigma$ . For fixed  $M$  and large  $R$  the wall velocity is directly related to the volume contribution proportional to  $\kappa^2 - 1/\ell_{\text{AdS}}^2 - 1/\ell_{\text{dS}}^2$ . The total volume effect can be negative or positive. As a result, it is possible for the total mass  $M$  to be negative. Alternatively, we can solve eq. (9) for  $M$ , with the result

$$2GM = 2Gm - \left( \frac{1}{\ell_{\text{AdS}}^2} + \frac{1}{\ell_{\text{dS}}^2} + \kappa^2 \right) R^3 + 2\epsilon_1 \kappa R^2 \left( 1 - \frac{2Gm}{R} + \frac{R^2}{\ell_{\text{AdS}}^2} + \dot{R}^2 \right)^{1/2}. \quad (11)$$

For  $\epsilon_1 = 1$ ,  $\dot{R} \ll 1$  and  $G \rightarrow 0$ , the above expression has a Newtonian interpretation: The mass  $M$  attributed to the bubble of AdS by an outside observer contains a volume term proportional to  $-(1/\ell_{\text{AdS}}^2 + 1/\ell_{\text{dS}}^2 + \kappa^2)$ . The contribution  $-(1/\ell_{\text{AdS}}^2 + 1/\ell_{\text{dS}}^2)$  corresponds to the difference in vacuum energy density between the interior and exterior of the bubble, while  $-\kappa^2$  reproduces correctly the gravitational self-energy of the wall. The expansion of the second term in eq. (11) produces the surface energy of the bubble, the interaction energy between the surface and the black hole of mass  $m$ , the surface-volume interaction energy and the kinetic energy of the wall [8].

The evolution of a bubble can be deduced through the solution of eq. (9). By squaring this equation twice, we can express the equation of motion for the bubble wall as the equation for the one-dimensional motion of a particle of constant ‘energy’ in an effective ‘potential’. For fixed values of  $\ell_{\text{AdS}}$ ,  $\ell_{\text{dS}}$ ,  $\kappa$ ,  $m$ , the ‘energy’ depends on the total mass  $M$  of the configuration. A multitude of wall trajectories are possible for various values of  $M$ , describing shrinking or expanding bubbles [8, 7]. A complete analysis is provided in appendices A-C. In general, for a given set of parameters there is a critical configuration that separates small bubbles that tend to collapse from large bubbles that tend to grow and engulf the external space. The mass  $M$  of these bubbles characterizes the energy barrier for transitions towards the deeper AdS vacuum. In the following section we focus on the dependence of the energy barrier on the mass parameter  $m$  of the central black hole.

### 3 The critical bubbles

We concentrate on the bubble evolution for  $\kappa^2 \ll 1/\ell_{\text{AdS}}^2$ . For vacuum energies and surface tension induced by the Higgs field  $h$  through its potential,  $\kappa^2 \sim (G\sigma)^2$  is suppressed by  $h^2/M_{\text{Pl}}^2$  relative to  $1/\ell_{\text{AdS}}^2$ . As a result, the scenario with  $\kappa^2 > 1/\ell_{\text{AdS}}^2$  can be realized only for values  $h \gtrsim M_{\text{Pl}}$ . Gravitational corrections to the potential become important at such scales, so that it is not possible to make firm predictions. Alternatively, one may

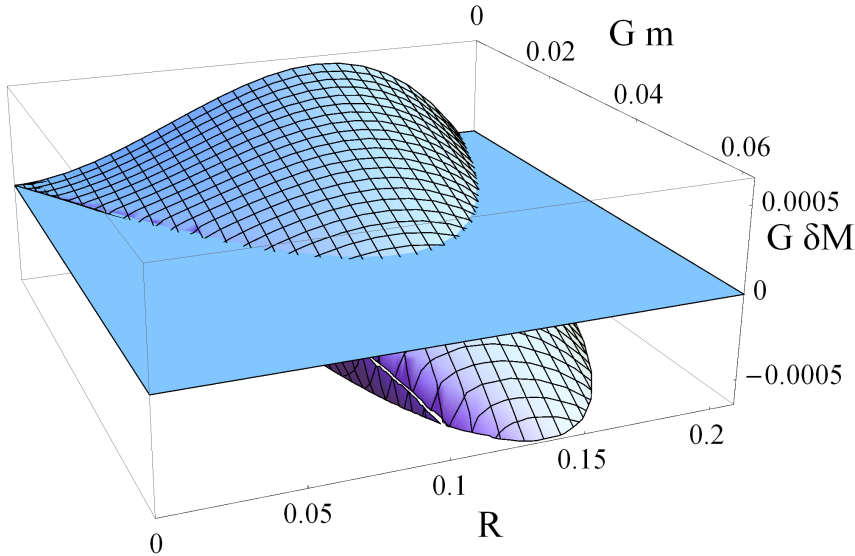


Figure 1: The mass difference  $\delta M = M - m$  for a bubble with  $\dot{R} = 0$  and  $\kappa = 0.1$ ,  $1/\ell_{\text{AdS}} \rightarrow 0$ , as function of its radius  $R$  and the mass  $m$  of the central black hole. All quantities are given in units of  $\ell_{\text{AdS}}$ .

assume that the Higgs field varies substantially over sub-Planckian distances. Such a scenario lacks predictivity also, as higher-derivative terms in the effective action become dominant. For these reasons, we focus our analysis on the case  $\kappa^2 \ll 1/\ell_{\text{AdS}}^2$ .

It is reasonable to assume that at the time of production of an AdS bubble the wall has small velocity. The reason is that the walls of the random field fluctuations do not have a preferred direction of motion. In the context of the spherical approximation, the assumption closest to the realistic scenario is that the bubbles are produced with little kinetic energy. For such bubbles there is a relation between their mass and radius, given by eq. (11) with  $\dot{R} = 0$ . For  $\epsilon_1 = 1$ , the resulting function  $M(R, m)$  has a maximum at  $R_{\text{max}}$ , corresponding to the critical bubble. Bubbles produced with  $R > R_{\text{max}}$  and  $\dot{R} = 0$  can only grow, while bubbles produced with  $R < R_{\text{max}}$  and  $\dot{R} = 0$  can only shrink. The value of  $M(R_{\text{max}}, m)$  can be used in order to estimate the energy barrier that must be overcome for growing bubbles to exist. It can be checked that the configurations with  $\epsilon_1 = -1$  in eq. (11) correspond to shrinking bubbles. (In fig. 1 we depict this branch as well, even though it is not relevant for our discussion below.)

For a central black hole with mass parameter  $m$ , the presence of an initially static AdS bubble of radius  $R$  results in the modification of the asymptotic ADM mass by an amount equal to  $\delta M(R, m) = M(R, m) - m$ . In fig. 1 we depict this function in units of  $\ell_{\text{AdS}}$  (i.e.  $\ell_{\text{AdS}} = 1$ ) for a Schwarzschild exterior ( $1/\ell_{\text{AdS}} \rightarrow 0$ ) and  $\kappa = 0.1$ . For  $m = 0$  the maximum corresponding to the critical bubble is clearly visible. It is also apparent that very large bubbles have  $M < 0$  because of the negative volume contribution. The presence of a central black hole with  $m > 0$  leads to the increase of the mass  $M$  of the

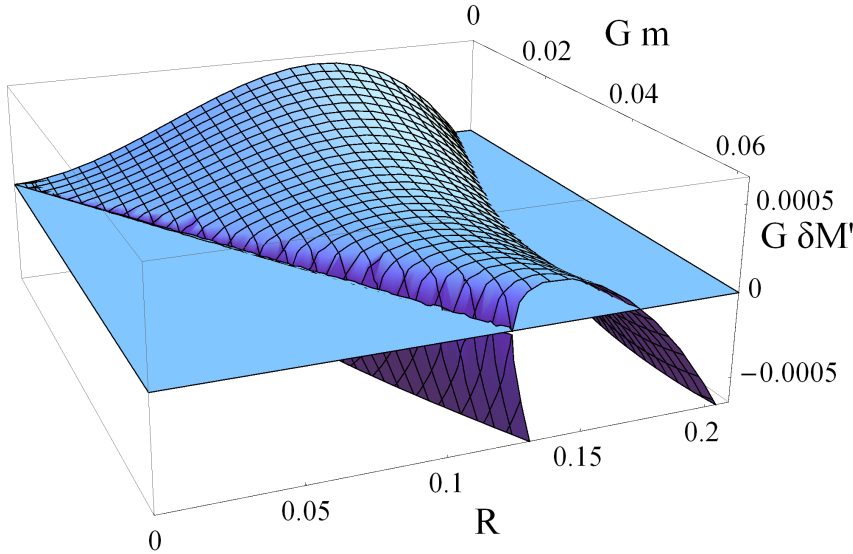


Figure 2: The mass difference  $\delta M' = M - R_h/(2G)$  for a bubble with  $\dot{R} = 0$  and  $\kappa = 0.1$ ,  $1/\ell_{\text{dS}} \rightarrow 0$ , as function of its radius  $R$  and the mass  $m$  of the central black hole. All quantities are given in units of  $\ell_{\text{AdS}}$ .

total configuration. However, the mass difference  $\delta M(R, m)$  is a decreasing function of  $m$ . There is a critical value  $m_{\text{cr}}$ , above which  $\delta M(R, m)$  is negative for all  $R$ . This value and the corresponding bubble radius  $R_{\text{cr}}$  can be obtained by requiring that  $\delta M(R_{\text{cr}}, m_{\text{cr}}) = \partial \delta M(R_{\text{cr}}, m_{\text{cr}})/\partial R = 0$ . We obtain

$$Gm_{\text{cr}} = \frac{1}{3}R_{\text{cr}} = \frac{2}{3\sqrt{3}} \frac{\kappa}{\left[\frac{1}{\ell_{\text{dS}}^2} + \left(\frac{1}{\ell_{\text{AdS}}} + \kappa\right)^2\right]^{\frac{1}{2}} \left[\frac{1}{\ell_{\text{dS}}^2} + \left(\frac{1}{\ell_{\text{AdS}}} - \kappa\right)^2\right]^{\frac{1}{2}}} \simeq \frac{2}{3\sqrt{3}} \frac{\kappa}{\frac{1}{\ell_{\text{AdS}}^2} + \frac{1}{\ell_{\text{dS}}^2}}. \quad (12)$$

The bubble radius  $R_{\text{cr}}$  is always larger than the horizon radius of the black hole.

Another characteristic feature of fig. 1 is the absence of bubbles with radii below a certain value. The perusal of eq. (11) reveals that, for  $\dot{R} = 0$ , the minimal radius  $R_h$  satisfies

$$1 - \frac{2Gm}{R_h} + \frac{R_h^2}{\ell_{\text{AdS}}^2} = 0. \quad (13)$$

It is clear that  $R_h$  coincides with the horizon of the AdS black hole of mass  $m$ . If the bubble is located within the horizon, with vanishing wall velocity, it cannot grow, as the attraction of the wall by the black hole is too strong. For  $2Gm/\ell_{\text{AdS}} \ll 1$  we have  $R_h \simeq 2Gm$ , while for  $2Gm/\ell_{\text{AdS}} \gg 1$  we have  $R_h \simeq (2Gm\ell_{\text{AdS}}^2)^{1/3}$ . A significant outward wall velocity allows bubbles with initial  $R < R_h$  to grow. However, we expect that the majority of bubbles are produced with small velocity.

The above analysis indicates that a black hole with mass larger than  $m_{\text{cr}}$  in asymptotically flat or dS space may not be separated by an energy barrier from a configuration



in which it is surrounded by an AdS bubble. However, the analysis cannot be considered rigorous because the mass parameter  $m$  is not a properly defined physical quantity. A geometrical quantity that can be used to characterize the energy content of the central region is the horizon radius  $R_h$ . The difference  $\delta M'(R, m) = M(R, m) - R_h(m)/(2G)$  provides an alternative estimate for the energy barrier associated with the bubble. Notice that  $R_h(m)/(2G)$  coincides with  $m$  only for  $2Gm/\ell_{\text{AdS}} \ll 1$ , while it is much smaller than  $m$  for  $2Gm/\ell_{\text{AdS}} \gg 1$ . As a result,  $\delta M'$  may provide an overestimate of the energy barrier for large  $m$ .

In fig. 2 we depict the function  $\delta M'(R, m)$  for bubbles with  $\dot{R} = 0$  and  $\ell_{\text{AdS}} = 1$ ,  $\kappa = 0.1$ ,  $1/\ell_{\text{dS}} \rightarrow 0$ . We observe the presence of a critical configuration for each value of  $m$ , similarly to fig. 1. The critical value of  $\delta M'$  initially drops as a function of  $m$ , but starts growing again for large  $m$ . The minimal critical value is obtained for values  $(R'_{\text{cr}}, m'_{\text{cr}})$  such that  $\partial \delta M'(R'_{\text{cr}}, m'_{\text{cr}})/\partial R = \partial \delta M'(R'_{\text{cr}}, m'_{\text{cr}})/\partial m = 0$ . An analytical expression for the solution of these equations can be obtained for small  $\kappa \ell_{\text{AdS}}$ . The full expression for nonzero  $1/\ell_{\text{dS}}$  is lengthy and not very illuminating. For this reason we present only the solution for  $1/\ell_{\text{dS}} \rightarrow 0$ , which reads

$$Gm'_{\text{cr}} = \frac{1 + \sqrt{13}}{12} R'_{\text{cr}} = \frac{\sqrt{16 - \sqrt{13}} (1 + \sqrt{13})}{36} \ell_{\text{AdS}}^2 \kappa. \quad (14)$$

The points  $(R_{\text{cr}}, m_{\text{cr}})$ ,  $(R'_{\text{cr}}, m'_{\text{cr}})$  are close, as can be seen from their approximate values:  $Gm_{\text{cr}} = R_{\text{cr}}/3 \simeq 0.385 \ell_{\text{AdS}}^2 \kappa$  and  $Gm'_{\text{cr}} = 1.151 R_{\text{cr}}/3 \simeq 0.450 \ell_{\text{AdS}}^2 \kappa$ .

The quantity  $\delta M'(R'_{\text{cr}}, m'_{\text{cr}})$  provides an estimate of the minimal energy barrier associated with the AdS bubble. For  $1/\ell_{\text{dS}} \ll 1/\ell_{\text{AdS}}$  we find a positive value, which can be compared with the barrier in the absence of the black hole, estimated by  $M(R_0, 0)$ , with  $\partial M(R_0, 0)/\partial R = 0$ . For small  $\kappa \ell_{\text{AdS}}$  and  $1/\ell_{\text{dS}} \rightarrow 0$ , we find

$$\frac{\delta M'(R'_{\text{cr}}, m'_{\text{cr}})}{M(R_0, 0)} = \frac{1}{32} \left( \sqrt{220 + 47\sqrt{13}} - \sqrt{1492 - 397\sqrt{13}} \right) \simeq 0.373. \quad (15)$$

We have verified this value through a numerical solution. The more conservative estimate of the energy barrier by  $\delta M'$  does not indicate complete instability. However, the presence of a black hole has a profound influence, as it can reduce the energy barrier by a factor of roughly 3. This has a strong effect on the nucleation rate, which is exponentially suppressed by the the energy barrier.

For  $1/\ell_{\text{dS}} \gg 1/\ell_{\text{AdS}}$  we have seen that  $\delta M$  for the critical bubble turns negative for a central black hole with a mass parameter given by eq. (12):  $Gm_{\text{cr}} \sim \kappa \ell_{\text{dS}}^2$ . As in this case  $2Gm_{\text{cr}} \ll \ell_{\text{AdS}}$ , we have  $2Gm_{\text{cr}} \simeq R_h$ . This means that  $\delta M'(R, m)$  also turns negative for a central black hole with this mass parameter, so that complete instability is expected for a strong dS background.

The fact that  $m_{\text{cr}}, m'_{\text{cr}}$  are roughly equal for  $1/\ell_{\text{dS}} \rightarrow 0$ , while for  $1/\ell_{\text{dS}} \gg 1/\ell_{\text{AdS}}$  the instability appears for a black-hole mass given by eq. (12), leads to the conclusion that

the critical mass can be estimated through the relation

$$Gm_{\text{cr}} \sim \frac{\kappa}{\frac{1}{\ell_{\text{AdS}}^2} + \frac{1}{\ell_{\text{dS}}^2}} \quad (16)$$

for all values of  $1/\ell_{\text{AdS}}$ ,  $1/\ell_{\text{dS}}$ .

## 4 Higgs (in)stability

In order to determine the relevance of our analysis for the fate of the Higgs field, we must recall some results for the Higgs potential in the Standard Model [7]: The Higgs potential has the approximate form  $V \sim \lambda(h)h^4/4$  for values of the Higgs field  $h$  above  $10^6$  GeV. The quartic coupling  $\lambda$  varies from 0.02 to  $-0.02$  for Higgs values between  $10^6$  GeV and  $10^{20}$  GeV, respectively. The maximum of the potential is located at a value  $h_{\text{max}} \sim 5 \times 10^{10}$  GeV. Near the maximum the potential can be approximated as [7]

$$V(h) \simeq -b \ln \left( \frac{h^2}{h_{\text{max}}^2 \sqrt{e}} \right) \frac{h^4}{4}, \quad (17)$$

with  $b \simeq 0.16/(4\pi)^2$ . For Higgs values within the range of interest around  $h_{\text{max}}$ , we have  $|\lambda| = \mathcal{O}(10^{-3})$ . In order to avoid the destabilization of the standard electroweak vacuum because of Higgs fluctuations during inflation, one requires that the scale  $H_{\text{inf}}$  of inflation satisfies  $H_{\text{inf}} \lesssim 0.04 h_{\text{max}}$  (for a minimally coupled Higgs field). When this constraint is satisfied the probability for the Higgs field to fluctuate beyond the maximum of the potential is exponentially small.

The presence of a black hole alters this picture drastically. If its mass is comparable to the critical value (16), the energy barrier to be overcome in order to produce an AdS bubble around a black hole is reduced significantly compared to the barrier in the absence of a black hole. Masses larger than  $m_{\text{cr}}$  are also relevant, because Hawking evaporation makes the black-hole mass scan a wide range of values during the cosmological evolution. It is, therefore, important to compare the specific value of  $m_{\text{cr}}$  for the Higgs potential with the maximal mass  $m_{\text{bh}} \sim M_{\text{Pl}}^2/H$  of primordial black holes produced at some given time during or after inflation. A precise determination of the bubble profile requires a numerical solution of the equation of motion for the Higgs field. Before presenting this solution, we discuss an estimate based on the thin-wall approximation of the previous sections, omitting factors of order 1.

We use rough estimates of the Higgs potential near  $h_{\text{max}}$  in terms of a positive parameter  $\hat{\lambda} = \mathcal{O}(10^{-3})$ . The energy density in the interior of a bubble is  $V \sim -\hat{\lambda}h^4$ . The surface tension can be estimated from the Newtonian expression

$$\sigma \sim \frac{h^2}{\Delta r} + \Delta r \hat{\lambda} h^4 \gtrsim \sqrt{\hat{\lambda}} h^3, \quad (18)$$

minimized for a bubble thickness  $\Delta r \sim 1/(h\sqrt{\hat{\lambda}})$ . The critical value (16) can now be compared to the maximal mass  $m_{\text{bh}} \sim M_{\text{Pl}}^2/H$  of a primordial black hole produced at a given time. We obtain

$$\frac{m_{\text{cr}}}{m_{\text{bh}}} \sim \frac{|V|}{V' + |V|} \frac{H}{\sqrt{\hat{\lambda}h}}, \quad (19)$$

with  $V \sim -\hat{\lambda}h^4$ , and  $V'$  equal to the inflaton vacuum energy  $V_{\text{dS}}$  during inflation, or to zero after its end.

- During inflation, the constraint  $H_{\text{inf}} \lesssim 0.04 h_{\text{max}}$  gives  $H_{\text{inf}}/(\sqrt{\hat{\lambda}h_{\text{max}}}) \lesssim 1$  for  $\hat{\lambda} = \mathcal{O}(10^{-3})$ , while we must have  $|V|/V' \ll 1$  for the positive vacuum energy to dominate. Thus we obtain

$$\frac{m_{\text{cr}}}{m_{\text{bh}}} \lesssim \frac{|V|}{V'} \frac{h_{\text{max}}}{h}. \quad (20)$$

For Higgs values within the bubble in the vicinity of  $h_{\text{max}}$ , the mass of the typical black hole is larger than the critical mass for the instability to appear.

- After the end of inflation,  $V' = 0$  and  $H^2 \sim \hat{\lambda}h^4/M_{\text{Pl}}^2$ , so that

$$\frac{m_{\text{cr}}}{m_{\text{bh}}} \sim \frac{h}{M_{\text{Pl}}} \quad (21)$$

and the maximal black hole mass is larger than  $m_{\text{cr}}$ . Black holes with masses that are a fraction of the maximal value fall within the region that induces the drastic reduction of the energy barrier.

Despite the absence of a significant energy barrier, the formation of an AdS bubble cannot proceed if its typical size is larger than the size of the causally connected regions in the Universe  $R_{\text{H}} \sim 1/H$ . From eq. (12) we have

$$\frac{R_{\text{cr}}}{R_{\text{H}}} \sim \frac{|V|}{V' + |V|} \frac{H}{\sqrt{\hat{\lambda}h}}. \quad (22)$$

As we discussed above, this ratio is smaller than one at all times.

## 5 Numerical solutions

The analysis of the previous sections is based on the thin-wall approximation, in which the transition from the interior AdS-Schwarzschild spacetime to the external asymptotically flat or dS spacetime takes place within a shell of very small width. Moreover, the vacuum energy is assumed to be constant on either side of the wall. In the realistic scenario, the Higgs field varies continuously as a function of the radius and the bubbles have large

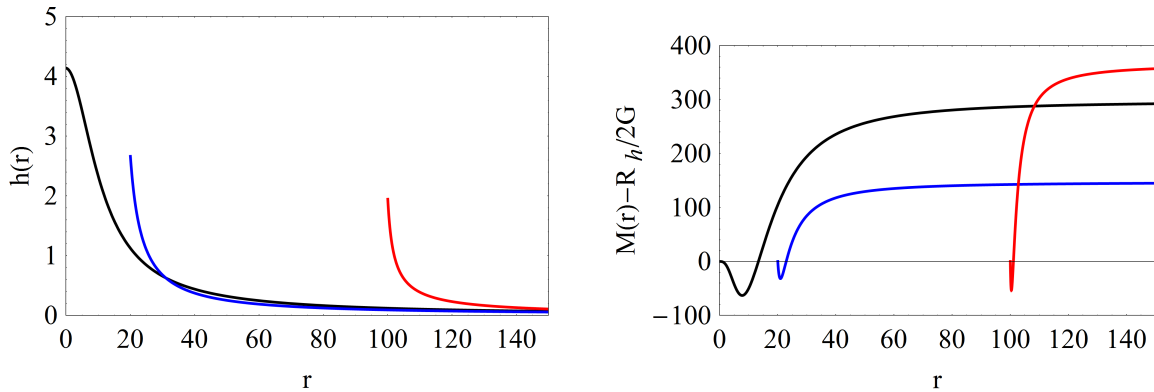


Figure 3: *The Higgs field  $h(r)$  (left plot) and the mass function  $M(r)$  (right plot) outside a black hole with horizon radius  $R_h = 0.1, 20$  and  $100$  (lines from left to right). All quantities are given in units of  $h_{\max}$ .*

thickness. The profile of the critical bubble can be obtained by solving the equation of motion of the Higgs field with appropriate boundary conditions that force the field to interpolate between values on either side of the maximum of the potential. As the critical bubble is static (but unstable) the corresponding field configuration has no time dependence. The ADM mass for this configuration quantifies the energy barrier that must be overcome for the field to fluctuate beyond the potential maximum. The nucleation rate is expected to be suppressed by this mass. The characteristic scale of the fluctuations, which determines the dispersion of the Higgs field, is set by the environment. If thermal equilibrium is assumed, the scale is given by the temperature. However, a high density environment with strong fluctuations also affects the Higgs field through the Yukawa couplings to the particles that contribute to the density.

The purpose of this first study is not to analyze a specific scenario, but to establish the effect of a black-hole background on the nucleation rate. For this reason, we concentrate on the role of black holes after the end of inflation, assuming an asymptotically flat spacetime. We also employ the zero-temperature Higgs potential, neglecting temperature or density corrections. A more focused analysis will be presented in the future. We solve numerically the Einstein and Higgs-field equations for the static critical bubbles, using the potential of eq. (17). We assume a metric of the form

$$ds^2 = -N(r) e^{2\delta(r)} dt^2 + N^{-1}(r) dr^2 + r^2 (d\theta^2 + \sin^2 \theta d\phi^2), \quad (23)$$

with  $N(r) = 1 - 2GM(r)/r$ . The equations of motion are reduced to

$$M' = 4\pi r^2 \left( \frac{1}{2} N h'^2 + V(h) \right) \quad (24)$$

$$\delta' = 4\pi G r h'^2 \quad (25)$$

$$h'' + \left( \frac{2}{r} - 8\pi G \frac{r}{N} V(h) + 2G \frac{M}{Nr^2} \right) h' = \frac{1}{N} \frac{dV(h)}{dh}, \quad (26)$$

with the prime denoting a derivative with respect to  $r$ .

The presence of the horizon at  $r = R_h$  requires the introduction of appropriate boundary conditions at this point. The function  $N(r)$  vanishes at  $r = R_h$ , which sets

$$2GM(R_h) = R_h. \quad (27)$$

In order to obtain a finite value for the ADM mass of the configuration we must avoid a singularity in eq. (26) at  $r = R_h$ . This can be achieved only if we impose

$$h'(R_h) = \frac{R_h}{1 - 8\pi G R_h^2 V(h(R_h))} \frac{dV(h(R_h))}{dh}. \quad (28)$$

Notice that this boundary condition correctly reproduces the standard condition  $h'(0) = 0$  in the absence of a black hole. We also require that

$$h(r) \rightarrow 0 \quad \text{for } r \rightarrow \infty \quad (29)$$

$$\delta(r) \rightarrow 1 \quad \text{for } r \rightarrow \infty. \quad (30)$$

With these conditions  $M(r)$  corresponds to the mass function of eq. (11) in the thin-wall approximation. We are interested in the quantity  $\delta M' = M(\infty) - R_h/(2G)$ , which corresponds to the similarly denoted quantity of section 3. It can be seen from eqs. (24), (27) that  $\delta M'$  results from the integration of the energy contributions associated with the bubble. It gives an estimate of the barrier associated with the production of the bubble around a central black hole with horizon radius  $R_h$ .

For the potential of eq. (17), the set of eqs. (24)-(25) has the trivial solution  $h(r) = 0$ ,  $M(r) = R_h/(2G)$ , and a nontrivial one with a characteristic scale set by  $h_{\max} \sim 5 \times 10^{10}$  GeV. The hierarchy between this scale and  $M_{\text{Pl}}$  makes the rhs of eq. (25) negligible. As a result, we have  $\delta = 1$  to a very good approximation in all the solutions we present.

In fig. 3 we depict the solutions for the Higgs field  $h(r)$  (left plot) and the quantity  $M(r) - R_h/(2G)$  (right plot) in the exterior of the black hole. We present three solutions for black holes with horizon radii  $R_h = 0.1, 20$  and  $100$  (lines from left to right). All quantities are given in units of  $h_{\max}$ . For bigger black holes the derivative of the Higgs field at  $r = R_h$  tends to become more negative (see eq. (28)). As a result, the Higgs can reach the origin starting from smaller initial values: the transition to the vicinity of the origin is faster for larger  $R_h$ . The quantity  $M(r) - R_h/(2G)$  is zero on the horizon, becomes negative initially because of the negative contribution from the potential, but quickly turns positive as the field moves through the maximum of the potential. For  $r \rightarrow \infty$  it approaches a constant value  $\delta M'$ . This asymptotic value has a dependence on  $R_h$  similar to the one we discussed in section 3. For  $R_h \rightarrow 0$  we have  $\delta M' = M_0$ , with  $M_0$  denoting the size of the energy barrier in the absence of a black hole. For nonzero  $R_h$ ,

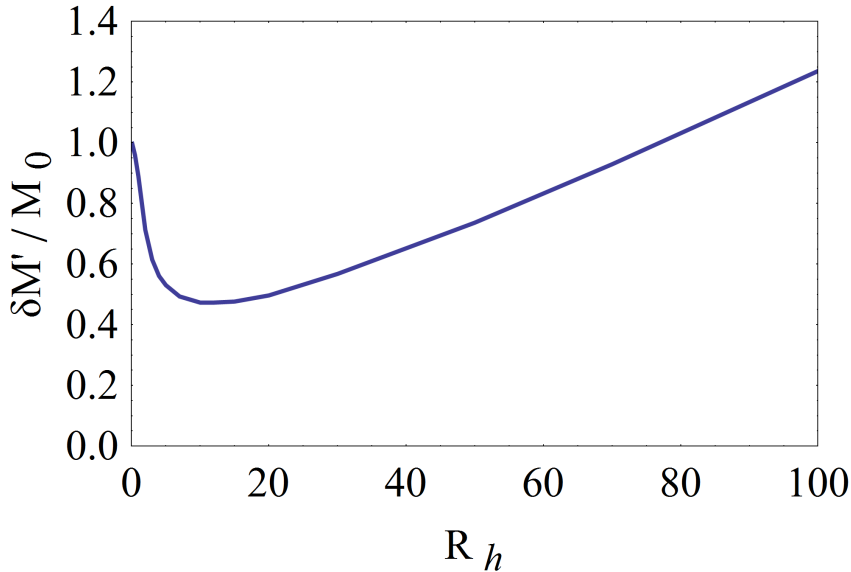


Figure 4: The ratio of the energy barrier in the background of a black hole relative to the barrier in the absence of a black hole.

$\delta M'$  initially decreases, as can be seen in fig. 3 for  $R_h = 20$ , but eventually grows, as can be seen for  $R_h = 100$ .

The ratio  $\delta M' / M_0$  denotes the relative size of the energy barrier in the background of a black hole with respect to the barrier in its absence. We depict it in fig. 4. We observe a minimum  $\delta M'_{\min} \simeq 0.473$  at  $R_h \simeq 11$ . This value can be compared to the result (15), derived through the thin-wall approximation. The small discrepancy is expected, as the numerical solutions for  $R_h \sim 10$  correspond to bubbles with significant wall thickness. There is a reduction of the energy barrier by approximately a factor of 2, instead of the factor of 3 indicated by eq. (15). However, this reduction still has a profound effect on the nucleation rate.

We conclude this section with some remarks on the properties of the solutions we presented:

- The characteristic scale of the solutions is set by  $h_{\max}$ . This means that gravitational corrections are not relevant, as they are suppressed by powers of  $h_{\max}^2 / M_{\text{Pl}}^2$ . Modifications are possible only if the Higgs potential receives corrections from new physics at scales close to  $h_{\max} \sim 10^{10-11}$  GeV.
- For our solutions  $\kappa \ell_{\text{AdS}} \sim \sqrt{G} h_{\max} \sim h_{\max} / M_{\text{Pl}} \ll 1$ . We have used this approximation in order to derive the various estimates in section 3.
- The energy  $\delta M'$  associated with the bubble is much smaller than the mass of the central black hole, as estimated by  $R_h / (2G)$ . This can be seen from the ratio  $G \delta M' / R_h \sim h_{\max}^2 / M_{\text{Pl}}^2$ . As a result, the gravitational background is induced mainly

by the black hole, with the bubble being only a small perturbation. This is the reason why the metric parameter  $\delta(r)$  equals 1 to a very good approximation.

## 6 Summary and conclusions

The general conclusion that can be reached through the analysis of sections 2 and 3 is that the presence of a black hole reduces the energy barrier for the destabilization of a false vacuum through classical fluctuations. The magnitude of the effect for the transition to an AdS vacuum depends on the quantity that one associates with the barrier. One may employ the difference  $\delta M = M - m$  between the ADM mass  $M$  of the black hole-bubble configuration and the mass parameter  $m$  of the black hole. In this case the barrier is completely eliminated for sufficiently large  $M$ , indicating complete instability. However, a quantity with a clearer physical meaning is the difference  $\delta M' = M - R_h/(2G)$ , with  $R_h$  the horizon radius. If  $\delta M'$  is employed in order to estimate the energy barrier, one must distinguish two cases: a) For an *asymptotically flat false vacuum*, the barrier is not completely eliminated in the presence of a black hole. However, an analysis based on the thin-wall approximation indicates that the barrier can be reduced by a factor of roughly 3. We point out that  $R_h/(2G)$  coincides with  $m$  only for  $2Gm/\ell_{\text{AdS}} \ll 1$ , with  $\ell_{\text{AdS}}$  the AdS length, while it is much smaller than  $m$  for  $2Gm/\ell_{\text{AdS}} \gg 1$ . As a result,  $\delta M'$  may provide an overestimate of the energy barrier for large  $m$ . b) For an *asymptotically dS false vacuum*,  $\delta M'$  turns negative for a sufficiently big black hole, indicating a complete instability.

The discussion of sections 2 and 3 is not specific to the potential of the Higgs field, as it is formulated only in terms of the energy density inside and outside the bubble, and the surface tension of the wall. When these are estimated from the Higgs potential (section 4), it becomes apparent that the presence of a typical primordial black hole has a profound effect on the energy barrier for classical transitions towards the region in which the potential becomes negative. The same is expected to be true for a wide range of potentials, resulting from physics beyond the Standard Model at zero and nonzero temperature, as long as the standard electroweak vacuum is metastable.

The calculation in section 5 of the exact bubble profile and the corresponding energy barrier for the Standard-Model Higgs in asymptotically flat space confirms the general picture, but also provides an estimate of the level of accuracy of the analysis of the earlier sections. In particular, it indicates that  $\delta M'$  can be reduced by an approximate factor of 2, instead of the approximate factor of 3 found in section 3. Even with this correction, the energy of the barrier  $\delta M'$ , when computed through the zero-temperature potential, drops from  $\sim 300$  to  $\sim 150$  in units of the Higgs value  $h_{\text{max}}$  at the maximum of the potential. The bubble nucleation rate per unit time scales proportionally to  $\exp(-\delta M'/T)$ . For temperatures  $T \sim h_{\text{max}}$ , for which the temperature corrections do not dominate the zero-temperature potential, the effect can be dramatic, with this factor being reduced from

$10^{-130}$  to  $10^{-65}$ . An analogous effect is expected at higher temperatures as well, but a precise analysis requires the use of the temperature-corrected potential.

The scenario in which primordial black holes, produced after inflation, induce the nucleation of bubbles of AdS vacuum is phenomenologically untenable. The expansion of the bubbles leads to catastrophic crunch singularities (see ref. [7] and appendices B and C), so that our visible Universe cannot develop. Whether this catastrophic scenario can be avoided depends strongly on the precise value of the energy barrier, but also on several other model-dependent factors, such as the rate of production of black holes and their typical mass.

The usual assumption is that primordial black holes can form after inflation when certain horizon-size overdense regions collapse gravitationally. The number of causally independent regions, that may have collapsed and are currently within our horizon, can be huge. The volume of our present horizon  $(3.4/H_0)^3$  gets suppressed by  $a^3$  at earlier times when the scale factor is  $a < 1$ . On the other hand, the volume of a horizon-size region during the radiation era is  $1/H^3$ . Therefore, the number of causally independent regions is roughly  $N \simeq a^3(3.4H/H_0)^3$ . The ratio  $H/H_0$  can be expressed as  $H/H_0 = \sqrt{g_*\Omega_\gamma/2(T/T_0)^2}$ , where  $g_* = 106.75$  is the number of degrees of freedom of the Standard Model,  $T_0 \simeq 2.4 \times 10^{-13}$  GeV the current photon temperature, and  $\Omega_\gamma \simeq 5 \times 10^{-5}$  the current energy fraction in photons. The scale factor  $a$  can be related to the temperature through entropy conservation:  $g_*T^3a^3 = g_{*S0}T_0^3$ , with  $g_{*S0} = 3.94$  the number of degrees of freedom contributing to the entropy after  $e^+e^-$  annihilation. Putting everything together gives  $N \sim 10^{34}(T/\text{GeV})^3$ . At a temperature  $T \sim h_{\text{max}} \sim 10^{11}$  GeV, we have  $N \sim 10^{67} \sim \exp(154)$ . If the primordial black holes are produced with sufficient probability, there is room for their effect to compensate the exponential suppression of the bubble nucleation rate. It should also be noted that Hawking evaporation makes the black-hole mass scan a wide range of values during the cosmological evolution, so that the energy barrier for the nucleation of AdS bubbles may vary with time through its minimal value.

The nucleation rate per unit time in the background of one black hole is  $dP/dt \sim T \exp(-\delta M'/T)$ . Notice that there is no volume factor, as the presence of the black hole eliminates the translational invariance. The characteristic time interval that can be associated with the scale  $T$  is the Hubble time  $1/H \sim M_{\text{Pl}}/T^2$ . The nucleation is efficient over longer times, but we are interested in a lower bound for the probability. Neglecting the evaporation of the black hole, we have a bubble-nucleation probability  $P \sim M_{\text{Pl}}/T \exp(-\delta M'/T)$ . For  $N$  causally independent regions, in each of which a primordial black hole can appear with probability  $p$ , the total nucleation probability becomes  $P \sim NpM_{\text{Pl}}/T \exp(-\delta M'/T) \sim p (T/10^{11})^2 \exp(173 - \delta M'/T)$ . When the barrier is reduced to  $\delta M'/T \simeq 150$ , as we discussed earlier, the exponential suppression is eliminated. It must be emphasized, however, that the probability  $p$  for the creation of a primordial black hole may be very small, resulting in the suppression of the rate.

It is clear from the above that the analysis of a detailed scenario requires the precise



determination of several physical parameters. In this work we identified a crucial factor in this discussion, namely the effect of the black-hole background on the height of the energy barrier for transitions to an AdS vacuum. In the most typical case, the transition to the AdS vacuum is induced by fluctuations within a Universe in thermal equilibrium. One may ask if the black holes that affect vacuum stability can be in equilibrium with the thermal background or affect it. For the black-hole masses of interest, this does not seem to be the case. As can be seen from fig. 4, the tunnelling rate becomes maximal for a black hole with Schwarzschild radius  $R_h \simeq 10/h_{\max}$  and Hawking temperature  $T_H \simeq h_{\max}/(40\pi)$ . We expect that the bubble nucleation rate will be most efficient for  $T \gtrsim h_{\max}$ . This means that the black holes are not in equilibrium, while they have only minor influence on the background. As a result, the main effect of the black holes on the critical bubbles is gravitational.

It must be kept in mind also that the Higgs field couples through the Yukawa couplings to particles that contribute to density fluctuations. This implies that the transition can take place in an environment that is out of thermal equilibrium if the density fluctuations are sufficiently strong. The temperature, or the Higgs-field dispersion induced by density perturbations, are additional model-dependent parameters whose time evolution must be calculated precisely in order to determine if the production of primordial black holes is consistent with our observable Universe.

## Acknowledgments

I would like to thank G. Giudice, A. Salvio, A. Strumia, A. Urbano for useful discussions.

## A Equation of motion

By squaring eq. (9) twice, we can express the result as the equation for the one-dimensional motion of a particle of total ‘energy’  $E$  in a ‘potential’  $V$ :

$$\left(\frac{d\tilde{R}}{d\tilde{\tau}}\right)^2 + V(\tilde{R}) = E, \quad (31)$$

with

$$V(\tilde{R}) = -\left(\frac{\epsilon_M - \zeta + \epsilon\tilde{R}^3}{\tilde{R}^2}\right)^2 - \epsilon_M \frac{\gamma^2}{\tilde{R}} - \delta^2 \tilde{R}^2, \quad E = -\frac{\kappa^2}{G^2 M^2 \rho^4}, \quad (32)$$

where

$$\Delta = \frac{1}{\ell_{\text{AdS}}^2} + \frac{1}{\ell_{\text{dS}}^2} - \kappa^2, \quad \rho^3 = \frac{1}{2G|M|} |\Delta|, \quad \gamma = \frac{2\kappa}{|\Delta|^{1/2}}, \quad \kappa^2 = \left(\frac{1}{\ell_{\text{AdS}}^2} + \frac{1}{\ell_{\text{dS}}^2}\right) \frac{\gamma^2}{\gamma^2 + 4\epsilon}, \quad \delta^2 = \frac{4\kappa^2}{\ell_{\text{dS}}^2 \Delta^2}, \quad (33)$$

and  $\epsilon = \text{sign}(\Delta)$ ,  $\epsilon_M = \text{sign}(M)$ ,  $\zeta = m/|M|$ . The dimensionless ‘coordinate’ variable  $\tilde{R}$  and the ‘time’ variable  $\tilde{\tau}$  are defined as  $\tilde{R} = \rho R$  and  $\tilde{\tau} = 2\kappa\tau/\gamma^2$ .

The form of the solutions of eq. (31) can be revealed more easily through the following observations:

- The sign  $\epsilon_2$  disappeared when performing the second squaring, so that eq. (31) describes the solutions of eq. (9) with both values of  $\epsilon_2$ . We can rewrite eq. (9) in terms of the new parameters as

$$\beta_{\text{in}} = \beta_{\text{out}} + 4\pi G\sigma R = \frac{G|M|\rho^2}{\kappa} \frac{1}{\tilde{R}^2} \left( \epsilon_M - \zeta + \epsilon \tilde{R}^3 + \frac{\gamma^2}{2} \tilde{R}^3 \right), \quad (34)$$

where we have used eq. (10). For growing bubbles with increasing  $\tilde{R}$ , we have  $\beta_{\text{in}} > 0$  (i.e.  $\epsilon_1 = 1$ ) after a sufficiently long time. This is obvious for  $\epsilon = 1$ . It also holds for  $\epsilon = -1$ , because  $\gamma^2 > 4$  in this case.

- We can also write

$$\beta_{\text{out}} = \frac{G|M|\rho^2}{\kappa} \frac{1}{\tilde{R}^2} \left( \epsilon_M - \zeta + \epsilon \tilde{R}^3 \right), \quad (35)$$

from which it is apparent that, for growing bubbles at late times, we have  $\beta_{\text{out}} > 0$  (i.e.  $\epsilon_2 = 1$ ) for  $\epsilon = 1$ , while  $\beta_{\text{out}} < 0$  (i.e.  $\epsilon_2 = -1$ ) for  $\epsilon = -1$ .

- For fixed  $\ell_{\text{AdS}}$ ,  $\ell_{\text{dS}}$  and  $\kappa$ , the total energy  $E$  is a function of  $M$ . As a result, the nature of the various solutions of eq. (31) is directly related to the mass of the bubble.
- The ‘potential’ has a maximum at  $\tilde{R} = \tilde{R}_{\text{max}}$ , given by

$$\tilde{R}_{\text{max}}^3 = \frac{\epsilon_M(2\epsilon + \gamma^2) - 2\epsilon\zeta + \sqrt{(\epsilon_M(2\epsilon + \gamma^2) - 2\epsilon\zeta)^2 + 32(1 + \delta^2)(\epsilon_M - \zeta)^2}}{4(1 + \delta^2)}. \quad (36)$$

In certain cases (e.g. for  $\epsilon_M = -1$ ,  $\delta = \zeta = 0$ ) the maximum of the ‘potential’ can be positive. The ‘potential’ then vanishes at

$$\tilde{R}_{1,2}^3 = \frac{-\epsilon_M(2\epsilon + \gamma^2) + 2\epsilon\zeta \pm \sqrt{\gamma^4 + 4\epsilon\gamma^2(1 - \epsilon_M\zeta) - 4\delta^2(\epsilon_M - \zeta)^2}}{2(1 + \delta^2)}. \quad (37)$$

- For  $\epsilon_M = 1$ , the horizon of the black hole of mass  $M$  seen by the external observer corresponds to a value  $\tilde{R}_{\text{H}}$  such that

$$E = -\frac{\gamma^2}{\tilde{R}_{\text{H}}} - \delta^2 \tilde{R}_{\text{H}}^2. \quad (38)$$

This relation determines the location of the horizon on a solution of eq. (31) with given  $E$ . Making use of the definition (32) of the ‘potential’, we can write

$$E = V(\tilde{R}_{\text{H}}) + \left( \frac{1 - \zeta + \epsilon \tilde{R}_{\text{H}}^3}{\tilde{R}_{\text{H}}^2} \right)^2. \quad (39)$$

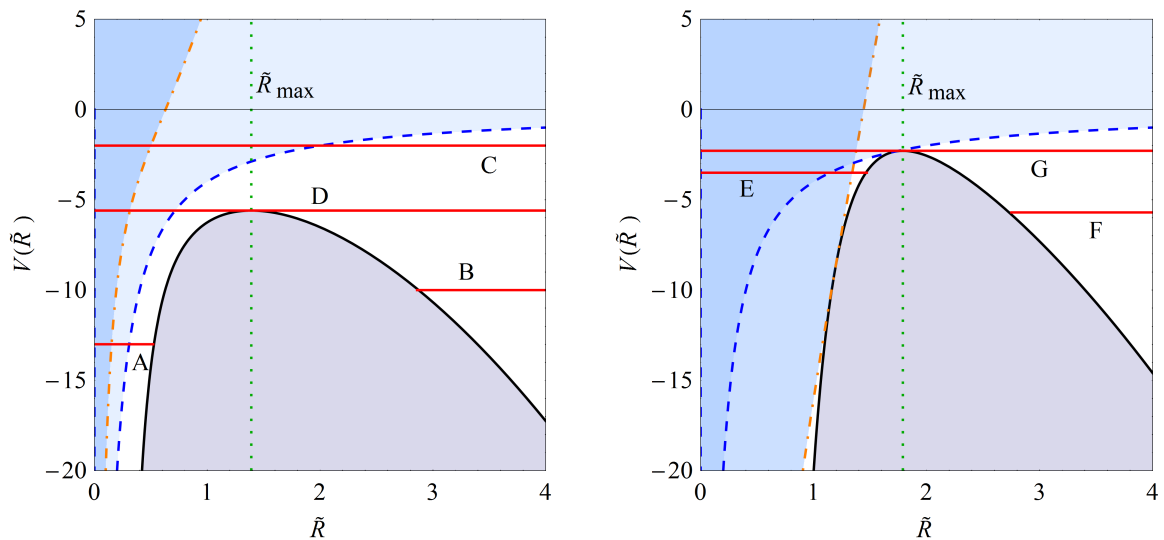


Figure 5: The ‘potential’ of eq. (32) for  $\epsilon_M = 1$ ,  $\gamma = 2$ ,  $\epsilon = 1$ ,  $\delta = 0$ ,  $\zeta = 0.5$  (left), and  $\epsilon_M = 1$ ,  $\gamma = 2$ ,  $\epsilon = 1$ ,  $\delta = 0$ ,  $\zeta = 6$  (right).

The curve  $-\gamma^2/\tilde{R} - \delta^2\tilde{R}^2$ , depicting the location of the horizon, is tangent to the curve  $V = V(\tilde{R})$  at

$$\tilde{R}^3 = \epsilon(\zeta - 1), \quad (40)$$

as long as this is positive. It is apparent from eq. (35) that  $\beta_{\text{out}}$  and  $\epsilon_2$  change sign at this point.

- The horizon of the AdS black hole of mass  $m$  corresponds to a value  $\tilde{R}_h$  such that

$$E = \left[ \frac{\gamma^2(\gamma^2 + 4\epsilon)}{4} - \delta^2 \right] \tilde{R}_h^2 - \frac{\zeta\gamma^2}{\tilde{R}_h}. \quad (41)$$

The curve depicting this horizon is tangent to  $V(\tilde{R})$  at

$$\tilde{R}^3 = \frac{2(\zeta - \epsilon_M)}{\gamma^2 + 2\epsilon}, \quad (42)$$

as long as this is positive. It is apparent from eq. (34) that  $\beta_{\text{in}}$  and  $\epsilon_1$  change sign at this point.

## B Bubble evolution in asymptotically flat space

We consider first the case of a bubble evolving in asymptotically flat space, which corresponds to  $\delta = 0$ . Possible solutions of eq. (31) are depicted in fig. (5) for positive

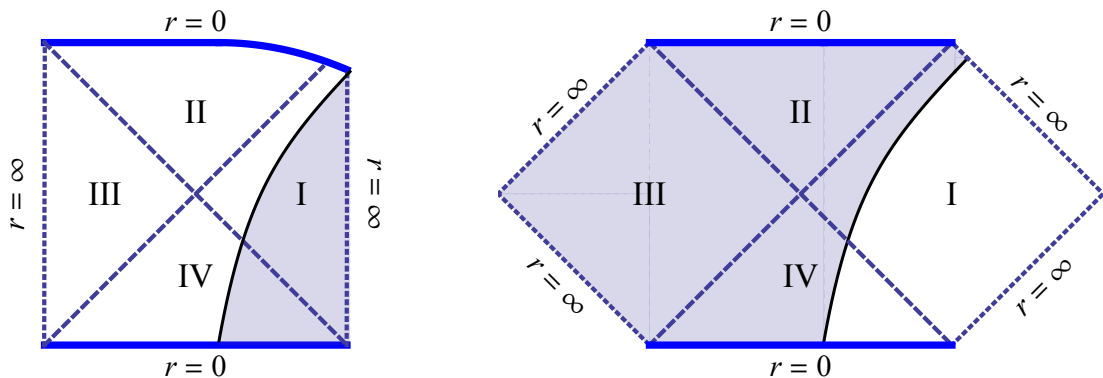


Figure 6: *The Penrose diagram for the wall trajectory  $C$  of fig. 5. The total spacetime is constructed by joining the two diagrams, after the elimination of the shaded areas.*

bubble mass  $M$  ( $\epsilon_M = 1$ ), and two values of the ratio  $\zeta = m/M$ . We have plotted the ‘potential’  $V(\tilde{R})$  and indicated the horizons of the internal (dot-dashed line) and external geometries (dashed line). The straight horizontal lines depict possible configurations of constant  $E$  and, therefore, bubble mass  $M$  seen by an outside observer. The lines A and E correspond to bubbles that expand from vanishing radius to a maximal size and then recollapse. During their evolution their walls cross the horizons. The lines B and F correspond to bubbles that start with infinite radius, shrink to a minimal size and then reexpand. Their walls are located outside both horizons. It is also possible for a bubble to be created spontaneously (with the appropriate wall velocity) at any point along the trajectories, and evolve from there. The lines D and G correspond to bubbles of critical mass. They have vanishing wall velocity and a radius corresponding to the location of the maximum of the ‘potential’. However, they are unstable, so that small deformations can lead to their expansion or collapse. The line C correspond to a bubble whose radius can vary continuously from vanishing to infinite as a function of time.

Penrose diagrams can be constructed, depicting the full spacetime for every type of wall trajectory. A typical example is shown in fig. 6, corresponding to the trajectory C of fig. 5. Thick blue lines denote curvature singularities, the dashed lines horizons and the dotted lines conformal infinities. The total spacetime is constructed by eliminating the shaded areas of the two diagrams and joining them along the wall trajectory. The bubble wall has initially vanishing radius, which grows with time. The wall crosses the

horizons of both the AdS-Schwarzschild (left) and Schwarzschild (right) geometries, and eventually reaches infinity.

The AdS interior is expected to be dynamically unstable [1]. For  $m = 0$ , the AdS space, when described in FRW coordinates, displays a coordinate singularity in a finite amount of internal time of order  $(G|V|)^{-1/2}$ . If the AdS space originates in a configuration of a background field (for example the Higgs field), the field fluctuations grow until the energy density becomes infinite and a physical singularity appears. Notice that both the AdS and AdS-Schwarzschild geometries have a timelike boundary, such that the evolution cannot be predicted after the bubble wall reaches the boundary, unless additional conditions are imposed there. As a result, a Cauchy horizon appears in the interior of the bubble. It is expected that, in the presence of a fluctuating field and beyond the thin-wall approximation, a physical spacelike singularity must develop before the Cauchy horizon [13]. For an AdS-Schwarzschild interior, this spacelike singularity is expected to merge with the spacelike singularity at  $r = 0$ . We have depicted the merging in fig. 6. The Penrose diagram supports the conclusion that the endpoint of the evolution of an expanding bubble is a catastrophic event. In the context of the Standard Model, such an event can be avoided by imposing an upper bound on the scale of inflation [7].

An interesting fact deduced from the second plot of fig. 5 is that there exist critical or expanding bubbles with  $\epsilon_M = 1$  and  $\zeta > 1$ . This means that the mass  $M$  assigned to the bubble configuration by an asymptotic observer is smaller than the mass parameter of the black hole  $m$ .

Several other types of Penrose diagrams can be obtained for the other trajectories depicted in fig. 5. They have been analyzed in detail in [7]. It is worth mentioning a particular class of spacetimes obtained for bubbles with large surface tension  $\kappa^2 > 1/\ell_{\text{AdS}}^2$  (or  $\epsilon = -1$ ). Despite the Newtonian intuition that such bubbles should not expand, general relativity allows the possibility of a bubble that grows behind an event horizon of the external geometry. A faraway observer sees only a localized defect in spacetime [8, 7]. We do not discuss such configurations in detail here, as our focus is on bubbles that lead to catastrophic events by engulfing the entire external space.

A different class of bubbles are characterized by negative mass  $M < 0$ . Such solutions are physically acceptable, as the would-be naked singularity at  $r = 0$  is eliminated by the interior of the bubble.<sup>1</sup> Typically, such bubbles have large radii and their energy is dominated by the negative energy density of the AdS interior. Two types of ‘potentials’ for  $M < 0$  (or  $\epsilon_M = -1$ ) are depicted in fig. 7. The ‘potential’ on the left corresponds to bubbles with relatively small surface tension ( $\epsilon = 1$  or  $\kappa^2 < 1/\ell_{\text{AdS}}^2$ ) and a rather small black hole at their center ( $\zeta = m/|M| = 0.5$ ). The maximum of the ‘potential’ has a positive value, which does not allow for solutions of the type C or D of fig. 5, because the ‘energy’  $E$  of the solutions is always negative (see eqs. (32)). The bubbles either shrink or expand, while there are no critical ones. The ‘potential’ on the right corresponds to

---

<sup>1</sup>In order to avoid naked singularities, we consider only internal geometries with  $m > 0$ .

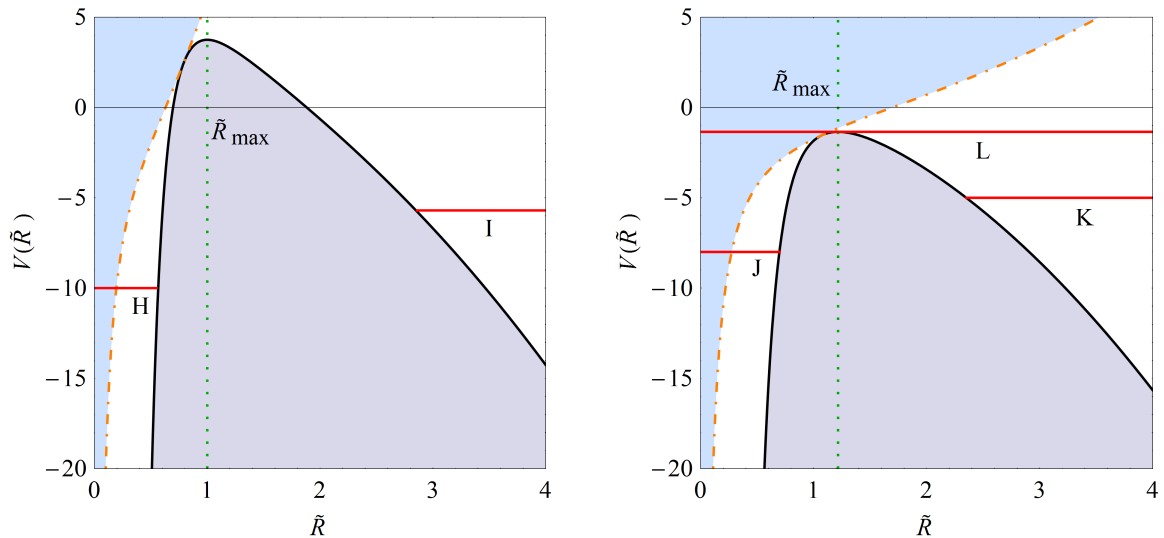


Figure 7: The ‘potential’ of eq. (32) for  $\epsilon_M = -1$ ,  $\gamma = 2$ ,  $\epsilon = 1$ ,  $\delta = 0$ ,  $\zeta = 0.5$  (left), and  $\epsilon_M = -1$ ,  $\gamma = 2.1$ ,  $\epsilon = -1$ ,  $\delta = 0$ ,  $\zeta = 0.5$  (right).

bubbles with large tension ( $\epsilon = -1$  or  $\kappa^2 > 1/\ell_{\text{AdS}}^2$ ), for which critical bubbles can exist. Notice that there is only one event horizon, that of the internal geometry.

A typical Penrose diagram, corresponding to the trajectories I and K of fig. 7 is depicted in fig. 8. The naked singularity in the diagram on the right is not relevant, as it is eliminated along with the shaded areas when the global spacetime is constructed.

## C Bubble evolution in asymptotically de Sitter space

We turn next to the case of a bubble evolving in asymptotically de Sitter space, which corresponds to  $\delta > 0$ . There are many possibilities depending on the signs of  $\epsilon$ ,  $\epsilon_M$ ,  $\epsilon_1$ ,  $\epsilon_2$ . We do not perform the complete analysis, as many cases are similar to those discussed in refs. [8, 7]. In fig. 9 we depict the ‘potential’ for some characteristic values of the various parameters for bubble configurations of positive mass  $M$ . The two plots correspond to black holes of mass  $m$  smaller ( $\zeta = m/M = 0.5$ ) or larger ( $\zeta = 6$ ) than  $M$ . We have plotted the ‘potential’  $V(\tilde{R})$  and indicated the horizon of the internal AdS-Schwarzschild geometry (dot-dashed line), as well as the horizons of the external dS-Schwarzschild geometry (dashed line). The straight horizontal lines depict possible configurations of constant bubble mass  $M$ . The line N corresponds to a bubble that expands from vanishing radius to a maximal size and then recollapses. During its evolution the wall crosses the horizon of the AdS-Schwarzschild geometry and the inner horizon of the dS-Schwarzschild geometry. The lines M and R correspond to bubbles that start

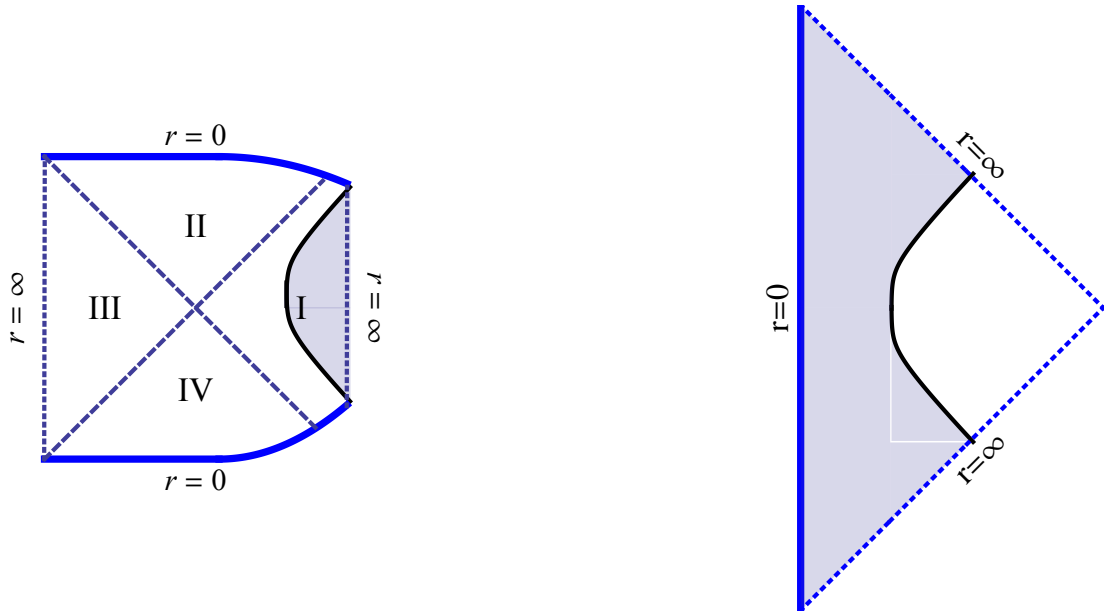


Figure 8: The Penrose diagram for the wall trajectories I and K of fig. 7. The total spacetime is constructed by joining the two diagrams, after the elimination of the shaded areas.

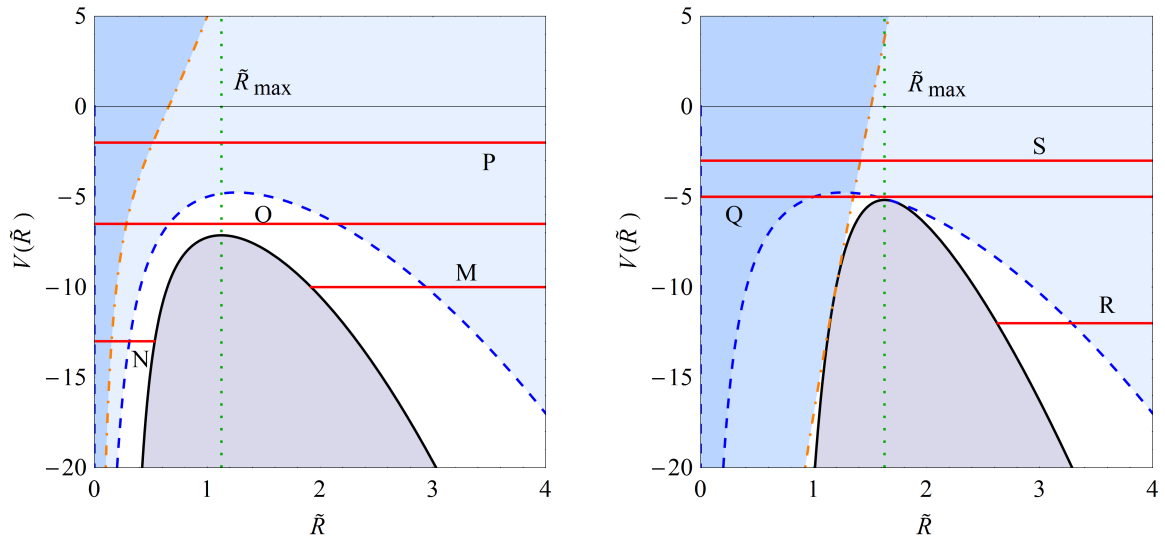


Figure 9: The ‘potential’ of eq. (32) for  $\epsilon_M = 1$ ,  $\gamma = 2$ ,  $\epsilon = 1$ ,  $\delta = 1$ ,  $\zeta = 0.5$  (left), and  $\epsilon_M = 1$ ,  $\gamma = 2$ ,  $\epsilon = 1$ ,  $\delta = 1$ ,  $\zeta = 6$  (right).

with infinite radius, shrink to a minimal size and then reexpand. Their walls cross only

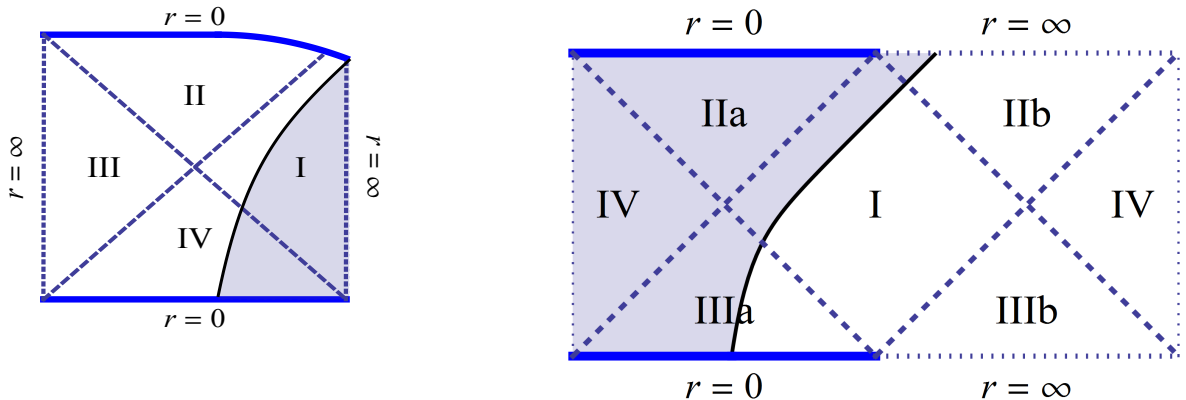


Figure 10: *The Penrose diagram for the wall trajectory O of fig. 9. The total spacetime is constructed by joining the two diagrams, after the elimination of the shaded areas.*

the outer horizon of the dS-Schwarzschild geometry. The lines O and Q correspond to bubbles whose radii can vary continuously from vanishing to infinite as a function of time. During their evolution they cross the horizon of the internal geometry, as well as the two horizons of the external geometry. The order in which these are crossed is different for the two configurations. Lines P and S correspond to bubbles whose wall crosses only the horizon of the AdS-Schwarzschild geometry. The reason is that ‘energies’ that approach zero correspond to large values of the mass parameter  $M$ . For sufficiently large  $M$ , the metric function  $f_{\text{out}}(r)$  stays always negative. The space has a naked spacelike singularity at  $r = 0$ . However, this part of space is eliminated and replaced by the interior of the AdS bubble.

In fig. 10 we present the Penrose diagram for the trajectory O of fig. 9. Thick blue lines denote curvature singularities, the dashed lines horizons and the dotted lines conformal infinities. The two thin vertical lines at the ends of the right diagram indicate that the pattern is repeated indefinitely on either side. A similar diagram corresponds to the trajectory Q. The wall of the expanding bubble crosses all three horizons and the bubble reaches infinite radius. The question whether the AdS bubbles can completely eliminate the surrounding dS space was addressed in ref. [7] in the absence of a central black hole. The conclusion is the same for an internal AdS-Schwarzschild geometry: It is apparent from fig. 10 that asymptotically the wall trajectory reaches spacelike infinity. The wall location separates two spacelike regions: the first corresponds to the interior of the bubble, while the second is part of an asymptotically dS spacetime. The total spacetime contains large AdS bubbles within large dS regions. In other words, expanding



bubbles are inflated away: they expand, but the dS space between them also grows. This scenario is in contrast to the case of asymptotically flat spacetime, in which the wall asymptotically reaches null infinity and the whole space is engulfed by the AdS bubbles.

Another important question concerns the consequences for an outside observer of the AdS ‘crunch’ in the bubble interior. This issue was also addressed in detail in ref. [7]. It was shown that the singularity never reaches the wall, as the latter expands with the speed of light. From the point of view of an external observer, the bubble just expands forever, within either de Sitter or Minkowski spacetime.

## References

- [1] S. R. Coleman and F. De Luccia, *Phys. Rev. D* **21** (1980) 3305.
- [2] G. W. Gibbons and S. W. Hawking, *Phys. Rev. D* **15** (1977) 2738.
- [3] J. R. Espinosa, G. F. Giudice and A. Riotto, *JCAP* **0805** (2008) 002 [arXiv:0710.2484 [hep-ph]]; G. Isidori, V. S. Rychkov, A. Strumia and N. Tetradis, *Phys. Rev. D* **77** (2008) 025034 [arXiv:0712.0242 [hep-ph]].
- [4] J. Elias-Miro, J. R. Espinosa, G. F. Giudice, G. Isidori, A. Riotto and A. Strumia, *Phys. Lett. B* **709** (2012) 222 [arXiv:1112.3022 [hep-ph]]; G. Degrassi, S. Di Vita, J. Elias-Miro, J. R. Espinosa, G. F. Giudice, G. Isidori and A. Strumia, *JHEP* **1208** (2012) 098 [arXiv:1205.6497 [hep-ph]]; D. Buttazzo, G. Degrassi, P. P. Giardino, G. F. Giudice, F. Sala, A. Salvio and A. Strumia, *JHEP* **1312** (2013) 089 [arXiv:1307.3536 [hep-ph]].
- [5] A. Kobakhidze and A. Spencer-Smith, *Phys. Lett. B* **722** (2013) 130 [arXiv:1301.2846 [hep-ph]]; arXiv:1404.4709 [hep-ph]; K. Enqvist, T. Meriniemi and S. Nurmi, *JCAP* **1310** (2013) 057 [arXiv:1306.4511 [hep-ph]]; M. Fairbairn and R. Hogan, *Phys. Rev. Lett.* **112** (2014) 201801 [arXiv:1403.6786 [hep-ph]]; K. Enqvist, T. Meriniemi and S. Nurmi, *JCAP* **1407** (2014) 025 [arXiv:1404.3699 [hep-ph]]; K. Kamada, *Phys. Lett. B* **742** (2015) 126 [arXiv:1409.5078 [hep-ph]]; A. Shkerin and S. Sibiryakov, *Phys. Lett. B* **746** (2015) 257 doi:10.1016/j.physletb.2015.05.012 [arXiv:1503.02586 [hep-ph]].
- [6] A. Hook, J. Kearney, B. Shakya and K. M. Zurek, *JHEP* **1501** (2015) 061 [arXiv:1404.5953 [hep-ph]]; M. Herranen, T. Markkanen, S. Nurmi and A. Rajantie, *Phys. Rev. Lett.* **113** (2014) no.21, 211102 [arXiv:1407.3141 [hep-ph]]; *Phys. Rev. Lett.* **115** (2015) 241301 [arXiv:1506.04065 [hep-ph]]; J. Kearney, H. Yoo and K. M. Zurek, *Phys. Rev. D* **91** (2015) 12, 123537 [arXiv:1503.05193 [hep-th]].
- [7] J. R. Espinosa, G. F. Giudice, E. Morgante, A. Riotto, L. Senatore, A. Strumia and N. Tetradis, *JHEP* **1509** (2015) 174 [arXiv:1505.04825 [hep-ph]].
- [8] S. K. Blau, E. I. Guendelman and A. H. Guth, *Phys. Rev. D* **35** (1987) 1747.
- [9] P. Burda, R. Gregory and I. Moss, *Phys. Rev. Lett.* **115** (2015) 071303 [arXiv:1501.04937 [hep-th]]; *JHEP* **1508** (2015) 114 [arXiv:1503.07331 [hep-th]]; arXiv:1601.02152 [hep-th].
- [10] Ya. B. Zeldovich and I. D. Novikov, *Sov. Astron. -AJ* **10** (1967) 602; S. Hawking, *Mon. Not. Roy. Astron. Soc.* **152** (1971) 75; B. J. Carr and S. W. Hawking, *Mon. Not. Roy. Astron. Soc.* **168** (1974) 399.

- [11] R. Bousso and S. W. Hawking, Phys. Rev. D **54** (1996) 6312 [gr-qc/9606052].
- [12] W. Israel, Nuovo Cim. B **44S10** (1966) 1 [Nuovo Cim. B **48** (1967) 463] [Nuovo Cim. B **44** (1966) 1].
- [13] B. Freivogel, G. T. Horowitz and S. Shenker, JHEP **0705** (2007) 090 [hep-th/0703146 [HEP-TH]].